2010 IEEE International Conference on Robotics and Automation
Anchorage Convention District
May 3-8, 2010, Anchorage, Alaska, USA

Online Methods for Radio Signal Mapping with Mobile Robots

Jonathan Fink and Vijay Kumar

Abstract— **In this paper we explore methods for the online mapping of received radio signal strength with mobile robots and localizing the source of the radio signal. By utilizing Gaussian processes, we are able to build an online model of the signal-strength map that can, in turn, be used to provide the current maximum likelihood estimate of the source location. Furthermore, using the estimate of the source location, the Gaussian process model allows for prediction of received signal strength with confidence bounds in regions of the environment that have not been explored. Finally, we develop a control law for collecting samples of the signal strength with mobile robots that allows for online estimation of the radio signal source.**

I. INTRODUCTION

Wireless communication is requisite in most multi-robot scenarios and devices for enabling wireless communication protocols through radio signals, such as *Zigbee*, *Bluetooth*, and *802.11*, are readily available and economically priced. It is well-known that environmental effects on radio signal propagation are significant and several models of radio signal propagation are discussed in [5], [9], [21], including: statistical, empirical direct-path, empirical multi-path, and ray optical models. In the robotics community, several works exploit the fact that radio-propagation is environment dependent by leveraging received signal strength indication (RSSI), a measurement of power present in a radio signal, as a model for localization, including [7], [12], [14]. This research suggests that it is possible to localize a robot in an environment by predicting the RSSI based on experimentally gathered or modeled data. In each of these works, the authors study communication via *802.11 b/g* or *Bluetooth*, with sampling in indoor environments via autonomous [12] or sparse manual [7], [14] methods. RSSI also plays an important role in multi-robot control algorithms which require inter-robot coordination via communication [16], [17]. The relationship between radio signal strength and bit error rate (and thus communication capability) is well studied and shown to be heavily correlated. Therefore, RSSI prediction is vital to the success of control algorithms requiring inter-robot communication.

We are interested in tasks that rely on the deployment of a team of networked robots into an environment for which we *do not* have an accurate radio signal propagation model. Here we focus on developing tools that allow for online estimation and mapping of received radio signal strength. Specifically, we consider the simplest scenario in which there is a static base station in an unknown location that is transmitting to one or more mobile robots. The mobile robot(s) must autonomously build a map of the received signal strength and localize the base station.

We proceed as follows. In Sec. II we detail some background material on radio signal propagation, Gaussian process methods, and active control for sensing. Section III provides some specifics for our experimental system and Sec IV then outlines our specific problem statement and solution approach. In Secs V and VI we conclude with results and future directions.

II. PRELIMINARIES

A. Radio Signal Propagation

Radio signal strength propagation is a complex multi-scale process. Received power is a function of distance from the source, shadowing due to obstacles, and multi-path phenomena that arise as a result of reflections and refractions. While spatially and temporally averaged behavior can be fit to deterministic fading models, small-scale fading can cause variations to received signal strength on the order of 5 dBm over small length scales. While small-scale fading can be modeled by complex ray-tracing methods [21], it is perhaps more readily represented probabilistically by a Rician (when there *is* line-of-sight) or Rayleigh (for non-line-of-sight) distributions. Thus, the received power (in dBm) can be given by

$$P_{\text{dBm}} = \underbrace{L_0 - 10n \cdot \log(\|x^s - x\|)}_{\text{Fading}} - \underbrace{f(x^s, x)}_{\text{Shadowing}} - \underbrace{\epsilon}_{\text{Multipath}} \quad (1)$$

where L_0 is the measured power at 1 m from the source, n is the decay exponent, and x^s, x are the positions of the source and receiver respectively, $f(\cdot,\cdot)$ is a non-smooth function that describes shadowing, and ϵ is drawn from a Rayleigh or Rician distribution.

Though (as shown in our previous work [8] and depicted in Fig. 1) a dense sampling of a particular environment can yield accurate parameter estimation, we wish to deploy our methods in unknown environments that can not be sampled a priori. Thus, we shall continue by describing a probabilistic framework that we can utilize for online learning and estimation of the radio signal mapping.

B. Gaussian Processes

Gaussian process methods allow us a probabilistically sound way to incorporate noisy measurements from an unknown process and then make predictions on the evaluation of the process at unknown states. Gaussian processes (GP) are used in many mobile robotics applications such as sensor-centric localization [3] and mapping gas dispersal [20].

J. Fink and V. Kumar are with the GRASP Laboratory, University of Pennsylvania, 3330 Walnut Street, Philadelphia, PA. {jonfink,kumar}@grasp.upenn.edu

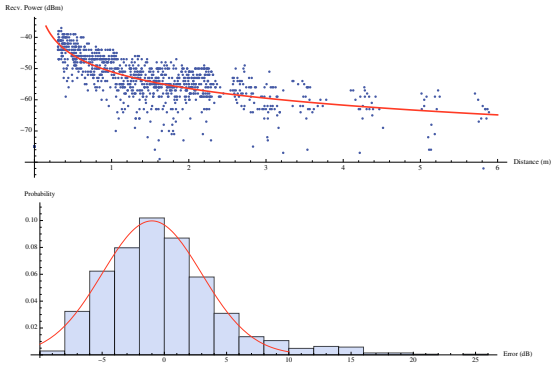

Fig. 1. Log-fading model fit to experimental data. Note that deviations from this mean function can be modeled by a Rician fading model or approximated by a non-zero-mean Gaussian

Radio signal strength is specifically considered in [7], where Ferris el al. demonstrate the utility of Gaussian processes for robotic localization tasks and continue in [6] by addressing the simultaneous localization and mapping problem when receiving transmissions from multiple base stations.

We will depart from [7] and [6] in two major ways. First, we will not assume that we have explored and sampled the environment a priori – we are primarily inerested in online methods that improve in quality as the environment is explored. Second, as a consequence of the requirement that we make signal strength predictions in unexplored regions, it is necessary to impose a model-based prior on the radio signal propagation. This introduces an additional complexity of parameter estimation that will be a primary focus of this work.

Here we will provide a brief introduction to the basic method adopting the function-space view defined in [18]. A Gaussian process describes a distribution over functions so that the mean function $\mu(x)$ and covariance function $k(x, x')$ of a process are

$$\begin{aligned} \mu(x) &= \mathbb{E}[f(x)] \\ k(x, x') &= \mathbb{E}[(f(x) - \mu(x))(f(x') - \mu(x'))], \end{aligned}$$

and the Gaussian process is then

$$f(x) \sim \mathcal{G}P(m(x), k(x, x')).$$

We will consider x to be a training point for which we have a corresponding measurement $y = f(x)$ and X to be a list of such training points. With subscript $*$, x_* denotes a point where we wish to sample the Gaussian process and obtain a prediction $f_* = f(x_*)$. Finally, the covariance (or kernel) function $k(x, x')$ can be applied to vectors so that $K(X, X')$ is the covariance matrix relating each pair of points.

If we assume a measurement model of the form $y = f(x) + \epsilon$ where $\epsilon \sim \mathcal{N}(0, \sigma_n^2)$, the covariance between measurements $\mathbf{y}$ at points X becomes

$$cov(\mathbf{y}) = K(X, X) + \sigma_n^2 I.$$

This leads to a joint distribution of the observed measurements and desired test locations to be

$$\begin{bmatrix} \mathbf{y} \\ \mathbf{f}_* \end{bmatrix} \sim \mathcal{N}\left(0, \begin{bmatrix} K(X, X) + \sigma_n^2 I & K(X, X_*) \\ K(X_*, X) & K(X_*, X_*) \end{bmatrix}\right).$$

Conditioning on the measurements, we obtain the predictive statements

$$\begin{aligned} \bar{f}_* &= \mathbb{E}[\mathbf{f}_* | X, \mathbf{y}, X_*] \\ &= \mathbf{k}_*[K(X, X) + \sigma_n^2 I]^{-1}\mathbf{y} \end{aligned} \tag{2}$$

$$\begin{aligned} \mathbb{V}[\mathbf{f}_*] =& k(x_*, x_*) \\ &- \mathbf{k}_*[K(X, X) + \sigma_n^2 I]^{-1}\mathbf{k}_*. \end{aligned} \tag{3}$$

where $\mathbf{k}_*$ is the vector of variances between x_* and each training point. Note that this assumes a zero-mean prior – below we will extend these equations to include a more descriptive prior on the mean function of the process.

We can also compute the log marginal likelihood of the model with respect to the training data to be

$$\begin{aligned} \log p(\mathbf{y}|X) = &-\frac{1}{2}\mathbf{y}^{\mathrm{T}}(K + \sigma_n^2 I)^{-1}\mathbf{y} \\ &-\frac{1}{2}\log|K + \sigma_n^2 I| - \frac{n}{2}\log 2\pi \end{aligned} \tag{4}$$

where K is used as shorthand for $K(X, X)$.

Initially, we shall adopt a squared exponential covariance function

$$k(x, x') = \sigma_f^2 \exp\left(-\frac{\|x - x'\|^2}{2\ell^2}\right).$$

Note that the parameters σ_f and ℓ control the shape of the covariance function and thus affect the behavior of the Gaussian process. ℓ models the length scale of variation and σ_f the amplitude of the variance. In general, the kernel parameters will be represented by a vector θ_k. It is not neccesary that the kernel function be stationary – it must only be positive semidefinite. In addition to a number of basis kernel functions, more complex functions can be formed by the addition or product of multiple kernel functions.

It will be useful in our work to specify an explicit prior on the mean function of the Guassian process that reflects the empirical model commonly used to model the fading of radio signal strength. In addition to other benefits, this enables more accurate prediction away from the training data. For a deterministic mean function $m(x)$, this modifies Eq. (2) to be

$$\begin{aligned} \bar{f}_* =& \mathbf{m}(x_*) \\ &+ \mathbf{k}_*[K + \sigma_n^2 I]^{-1}(\mathbf{y} - \mathbf{m}(X)). \end{aligned} \tag{5}$$

The covariance on predictions remains the same as (3). Note that like the kernel function, the mean function $m(x)$ can be characterized by a vector of parameters θ_m.

As stated above, both the covariance (or kernel) functions and the explicit prior on the mean function can be defined with respect to a set of parameters θ_k and θ_m respectively. These are often refered to as the hyperparameters of the Gaussian process and control how it fits the observations.

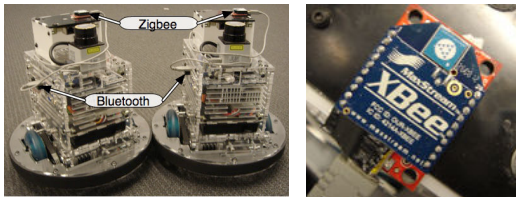

(a) (b)

Fig. 2. Two *Scarab* robots (Fig. 2(a)). Each robot is equipped with a *MaxStream XBee Zigbee* adapter (Fig. 2(b)).

Further, using the log marginal likelihood, we can perform an optimization to tune hyperparameters to our observed data. However, as seen later, there are several cases in which there are multiple local maxima in the log marginal likelihood that relate to different interpretations of the data and some may lead to over fitting.

C. Active Control

The concept of active control for information gain is clearly applicable to this work as we would like the mobile robot to efficiently gather samples that build a signal strength map with strong predictive capabilities. In [10], Grocholsky presents the idea of probabilistic information gain as a control objective which is applied in [11] to the problem of range-only localization.

In [13] Krause et al. study the issue of active sampling to build a Gaussian process with a key result that provides a theoretical condition for switching between exploration and exploitation strategies.

III. EXPERIMENTAL TESTBED

Before we describe the methodology and algorithms used in the paper, it is useful to discuss the experimental testbed and the hardware used in the experiments. In all experiments described in Secs. IV and V, a single stationary node transmits data via a *Zigbee* radios while a mobile robot controls autonomously through an indoor hallway and laboratory environment.

The robots and communication hardware used in the experiments are shown in Fig. 2. The *Scarab* is a $20 \times 13.5 \times 22.2$ cm^3 indoor ground platform. Each *Scarab* is equipped with a differential drive axle placed at the center of the length of the robot with a 21 cm wheel base, onboard computation, and *802.11a* wireless communication. Note that the operational frequency of *802.11a* is 5 GHz and all data logging and experiment monitoring occurred via this alternative frequency to avoid affecting the measurement of RSSI.

A Hokuyo URG 04-LX laser range finder and odometry information provide the necessary sensor information for laser-based localization in the environment. The *Zigbee* device is the *MaxStream XBee* as pictured in Fig. 2(b) with 1 mW (0 dBm) power output and receiver sensitivity of -92 dBm [1].

IV. METHODOLOGY

A. Problem Statement

We seek to develop online methods for mapping signal strength in unexplored environments. For this work we will assume (1) a stationary node periodically transmitting packets with unknown localization and (2) a mobile robot or team of mobile robots that share information, each of which has localization capabilities and the ability to navigate in the, possibly complex, environment. Given that the mobile robot can perform localization and receive radio broadcasts, it makes measurements $z_k = \begin{bmatrix} x_k, & y_k \end{bmatrix}$ consisting of a two-dimensional position $x \in \mathbb{R}^2$ and received signal strength y.

A Gaussian process is well suited to incorporate measurements and provide a predictive mapping from position to signal strength but, as stated above, it is essential that we incorporate a model-based prior to improve the quality of predictions in spatial regions where we have not captured measurements. A consequence of the introduction of a model-based prior is the addition of hyperparameters θ_m that must be estimated in addition to those for the kernel function θ_k.

Potential priors for the radio signal propagation are

$$m_1(x) = -L0, \tag{6}$$

$$m_2(x) = -L_0 - 10n\log_{10}(\|x^s - x\|), \tag{7}$$

$$m_3(x, \mathbf{d}) = -L_0 - 10n\log_{10}(\|x^s - x\|) + \sum_i k_i d_i. \tag{8}$$

Clearly, these functions require varying amounts of information about the source location and environment and can be interchanged depending on the problem statement. By incorporating more knowledge of the system, we can use more complex priors on the mean function of the Gaussian process (moving from m_1 to m_3 in Eq. 6-8) as depicted in Fig. 3. While the predictive mean of the Gaussian process near training points is unchanged, the marginal log likelihood from Eq. 4 increases and the predictions away from training data become more accurate. While $m_3(x)$, with its consideration of shadowing due to obstacles, is clearly the most descriptive, in this work we will limit ourselves to $m_2(x)$ to reduce the parameters that must be estimated.

Estimation of hyper-parameters θ_k and θ_m plays a crucial role in the effectiveness of the Gaussian process to provide probabilistically correct predictions. We shall see that the marginal log likelihood from Eq. 4 can be leveraged to find maximum likelihood estimates for the hyper-parameters.

Considering a mean function prior such as the log fading model $m_2(x)$ and a squared-exponential kernel function, the hyper-parameters are explicitly

$$\theta_k = \begin{bmatrix} \sigma_f^2 & \ell \end{bmatrix} \text{ and} \tag{9}$$

$$\theta_m = \begin{bmatrix} L_0 & n & x_1^s & x_2^s \end{bmatrix}. \tag{10}$$

While reasonably accurate priors can be determined for kernel parameters θ_k based on the small-scale fading phenomena and for mean function parameters L_0 and n, the model is

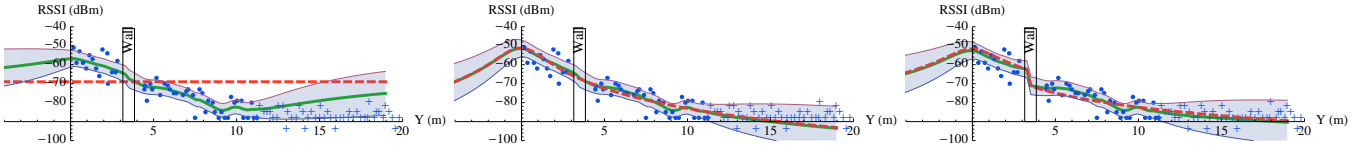

(a) $m_1(x) \Rightarrow \log\, p(\mathbf{y}|X) = -290$ (b) $m_2(x) \Rightarrow \log\, p(\mathbf{y}|X) = -259$ (c) $m_3(x) \Rightarrow \log\, p(\mathbf{y}|X) = -252$

Fig. 3. Gaussian process with 1D training data for $m_1(x)$ in Fig. 3(a), $m_2(x)$ in Fig. 3(b), and $m_3(x)$ in Fig. 3(c). The red dashed line indicates the mean function prior, blue points are the training data, and green solid is the Gaussian process predictive mean with associated variance depicted as an envelope around the mean. Note that blue crosses represent measurements not used as training data but provided here to demonstrate the quality of the signal strength prediction.

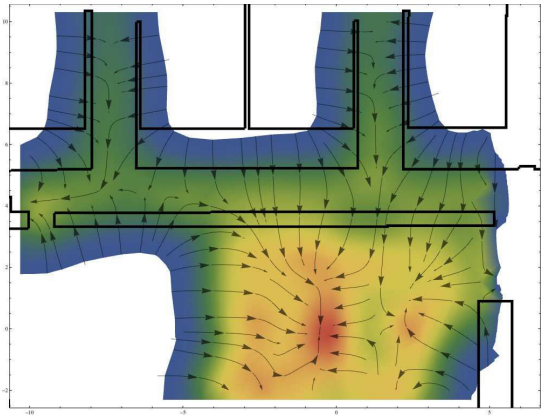

Fig. 5. If samples densly cover the domain, the Gaussian process provides a good model of the signal strength behavior without any mean function prior and can clearly be used to estimate the source location.

quite sensitive to the source location x^s which may be unbounded for an unknown environment. Figure 4 demonstrates the effect of source location on both the likelihood $p(\mathbf{y}|X)$ and the prediction in regions without training data.

B. Mapping using a dense sampling of the environment

In a set of preliminary experiments, we had a single robot exhaustively explore the environment taking measurements at 5Hz. Given a sufficiently dense sampling of the space around the source, it is possible to estimate the gradient of the signal strength map and follow it to the global maximum as depicted in Fig. 5. However, we wish to avoid having to explore the whole environment exhaustively and thus we shall first focus on a maximum likelihood estimator for the signal source location and continue to define a control law that incorporates both exploration of the space and exploitation based upon current estimates.

C. Maximum Likelihood Estimate of Signal Source

Given a parametric mean function that incorporates the signal source location, the marginal log-likelihood function

$$\mathcal{L}(\theta_m) = \log p(\mathbf{y}|X, \theta_m)$$

for a set of training data X is then

$$\begin{aligned}\log\, p(\mathbf{y}|X,\theta_m) = \\ -\frac{1}{2}(\mathbf{y}-m(X,\theta_m))^{\mathrm{T}}(K+\sigma_n^2 I)^{-1}(\mathbf{y}-m(X,\theta_m)) \\ -\frac{1}{2}\log|K+\sigma_n^2 I| - \frac{n}{2}\log 2\pi.\end{aligned} \tag{11}$$

In order to consider the maximum likelihood estimate $\hat{\theta}_m$ of the mean function parameters θ_m, we consider the gradient of the log-likelihood $\partial\mathcal{L}(\theta_m)/\partial\theta_m$

$$\begin{aligned}\frac{\partial\mathcal{L}(\theta_m)}{\partial\theta_m} &= \frac{\partial \log p(\mathbf{y}|X,\theta_m)}{\partial\theta_m} \\ &= (\mathbf{y}-m(X,\theta_m))^{\mathrm{T}}(K+\sigma_n^2 I)^{-1}\frac{\partial m(X,\theta_m)}{\partial\theta_m} \\ &= \left(\frac{\partial m(X,\theta_m)}{\partial\theta_m}\right)^{\mathrm{T}}(K+\sigma_n^2 I)^{-1}(\mathbf{y}-m(X,\theta_m))\end{aligned} \tag{12}$$

and perform gradient ascent to find $\hat{\theta}_m$. Note that if we assume to know the kernel parameters, this optimization can be evaluated with a single computation of the inverse $(K+\sigma_n^2 I)^{-1}$ which avoids the typically prohibitive $O(n^3)$ cost.

Furthermore, as shown in [2] we can use the second derivative of the log-likelihood

$$\begin{aligned}\frac{\partial^2\mathcal{L}(\theta_m)}{\partial\theta_{m,i,j}} = \\ \left(\frac{\partial^2 m(X,\theta_m)}{\partial\theta_{m,i,j}}\right)^{\mathrm{T}}(K+\sigma_n^2 I)^{-1}(\mathbf{y}-m(X,\theta_m)) - \\ \left(\frac{\partial m(X,\theta_m)}{\partial\theta_{m,i}}\right)^{\mathrm{T}}(K+\sigma_n^2 I)^{-1}\frac{\partial m(X,\theta_m)}{\partial\theta_{m,j}}\end{aligned} \tag{13}$$

to compute the Fisher information matrix

$$\mathcal{I}_{i,j} = -\frac{\partial^2\mathcal{L}(\theta_m)}{\partial\theta_{m,i,j}} \tag{14}$$

which, via the Cramer-Rao bound, provides a lower bound on the covariance of the maximum likelihood estimate $\hat{\theta}_m$ so that we can consider

$$\theta_m \sim \mathcal{N}(\hat{\theta}_m, \Sigma_m) \quad \text{where} \quad \Sigma_m = \mathcal{I}^{-1}. \tag{15}$$

D. Control Law

Our focus is on using a mobile robot to continously drive through an environment and sample the signal strength. We assume that signal strength mapping is the only task assigned to the robot so that it has full freedom to choose control directions that are most informative with respect to signal strength mapping. Here we take an exploration-exploitation approach similar in spirit to [13]. When we first enter an environment and have very few training samples, the estimate of θ_m is poor or sometimes impossible to determine, random exploration is the best/only strategy. However, when

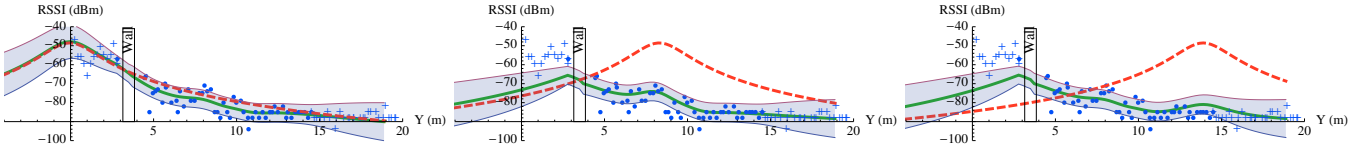

(a) $x^s = \{0, 0\} \Rightarrow \log\, p(\mathbf{y}|X) = -203$ (b) $x^s = \{0, 8\} \Rightarrow \log\, p(\mathbf{y}|X) = -305$ (c) $x^s = \{0, 14\} \Rightarrow \log\, p(\mathbf{y}|X) = -316$

Fig. 4. Similar to Fig. 3, here we depict the effect of mean function hyperparameters θ_m (specifically source location x^s) for $m_2(x)$. Note the actual source location is $x^s = \{0, 0\}$. Blue crosses are experimental data *not* input to the GP but provided to show the quality of the prediction.

an estimate is available for θ_m (particularly the source location), the controller can choose directions that are more informative.

To formalize, we define two control directions $\mathbf{u}_{explr}$ and $\mathbf{u}_{explt}$. The exploration direction $\mathbf{u}_{explr}$ is chosen to locally reduce the entropy of the Gaussian process by following the gradient of the predictive variance

$$\begin{aligned} \mathbf{u}_{explr}(x_*) &= \alpha_1 \nabla \mathbb{V}[f(x_*)] \\ &= \alpha_1 \left(\frac{\partial k(x_*, x_*)}{\partial x_*} - 2 \frac{\partial \mathbf{k}_*{}^{\mathrm{T}}}{\partial x_*} Q \mathbf{k}_* \right) \end{aligned}$$

where $Q = (K + \sigma_n I)^{-1}$. On the other hand, the exploitation direction is chosen based on the current maximum likelihood estimate of the source location $\hat{x}^s$

$$\mathbf{u}_{explt}(x_*) = \alpha_2 (\hat{x}^s - x_*).$$

The intuition behind this control direction for estimating the parameters of a log-based function is that samples must be collected away from the long flat tail of the function where the local variation will be within that explained by small-scale fading.

When a control direction $\mathbf{u_k}$ is chosen, the robot attempts to control along that direction for a fixed distance based upon the kernel parameters θ_k so that statistically independent samples can be collected. After the completion of each control action, $\mathbf{u_{k+1}}$ is chosen randomly to be either $\mathbf{u}_{explr}$ or $\mathbf{u}_{explt}$. The first control direction $\mathbf{u_0}$ is selected randomly since we have no prior knowledge or samples.

V. RESULTS

In Fig. 5, the signal strength prediction is depicted from a Gaussian process trained offline on samples that densely cover the complex indoor environment. In the results that follow we first demonstrate that the controller defined in Sec. IV-D can be used to efficiently localize a source and thus obtain an accurate prior for the remainder of the mapping process. We continue by demonstrating our method on a more complex environment and showing the accuracy of the resulting signal-strength map.

With respect to the online aspect of our work, it should be noted that we currently utilize a "standard" Gaussian process implementation in C++ that allows for realtime performance of the calculations we present here with hundreds of training points on a 2.5Ghz processor. However, there are a number of sparse approximations to Gaussian processes published [4], [15], [19] that allow for efficient operation as we increase the number of training points.

1) Open environment with active control: Here we place a stationary robot randomly in an open environment and have it broadcast packets via its *Zigbee* radio at 2 Hz. A mobile robot is started somewhere in the same obstacle-free region and follows the controller defined in Sec. IV-D as depicted in Fig. 6. After a random initial control direction in Fig. 6(a), there is an estimated source location in the $+x$-direction and the $\mathbf{u}_{explt}$ action is selected in Fig. 6(b). Figure 6(c) and 6(d) depict the $\mathbf{u}_{explr}$ control action while Figs. 6(e) and 6(f) depict execution of $\mathbf{u}_{explt}$.

Note that as samples are collected, multiple local maxima of the likelihood function $\mathcal{L}(\theta_m)$ (Fig. 6(e)) are resolved to the true maximum shown in Fig. 6(f). With an accurate estimate of the signal source location, we can use the Gaussian process to predict the signal strength at other locations. A variance associated with the prediction will represent confidence. Obviously, prediction confidence decreases away from sampled locations.

2) Complex Environment: In a complex hallway environment, allowable control directions are limited, precluding the use of the control law defined in Sec. IV-D. Instead, here we perform an explicit exploration by driving the length of the hallway in the x-direction as depicted in Fig. 7(a), predicting the source location (Fig. 7(b)), and comparing the resulting prediction to data gathered along the orthogonal hallway (Fig. 7(c)). Finally, Fig. 7(d) depicts a key strength of our GP-based approach. The source has been correctly localized but the gathered data is consistently different (as result of non-line-of-sight transmission). As the new data is included, the prediction improves.

VI. CONCLUSION & SUMMARY

We have presented a method for online mapping of radio signal strength from a static source at an unknown location using Gaussian processes which can provide not only predictive capabilities but also an associated uncertainty with each prediction. As our method relies on a model-based prior, we addressed the online estimation of model parameters – specifically the signal source location. By optimizing on a marginalized likelihood function and using an active control law, we are able to efficiently gather samples to estimate the signal source location. Additionally, we demonstrated the utility of our mapping technique in a complex environment including its ability to handle situations where the model-based prior is not sufficiently descriptive of the underlying process.

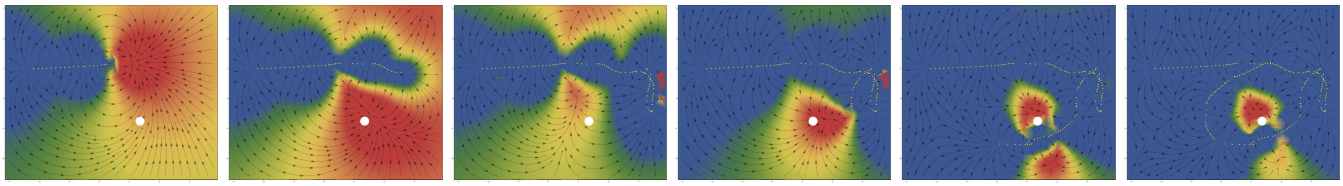

(a) $n = 20$ (b) $n = 38$ (c) $n = 73$ (d) $n = 85$ (e) $n = 112$ (f) $n = 155$

Fig. 6. The evolution of the likelihood function $\mathcal{L}(\theta_m)$ with respect to the signal source location x^s after n samples. As the experiment progresses from Fig. 6(a)–6(f), the measurements are incorporated into the Gaussian process, affecting the likelihood of the source location. The trial concludes when there is a clear global maximum of the likelihood function. Samples are represented by yellow points, the vector field depicts the gradient of $\mathcal{L}(\theta_m)$. The white circle in each figure represents the actual signal source location.

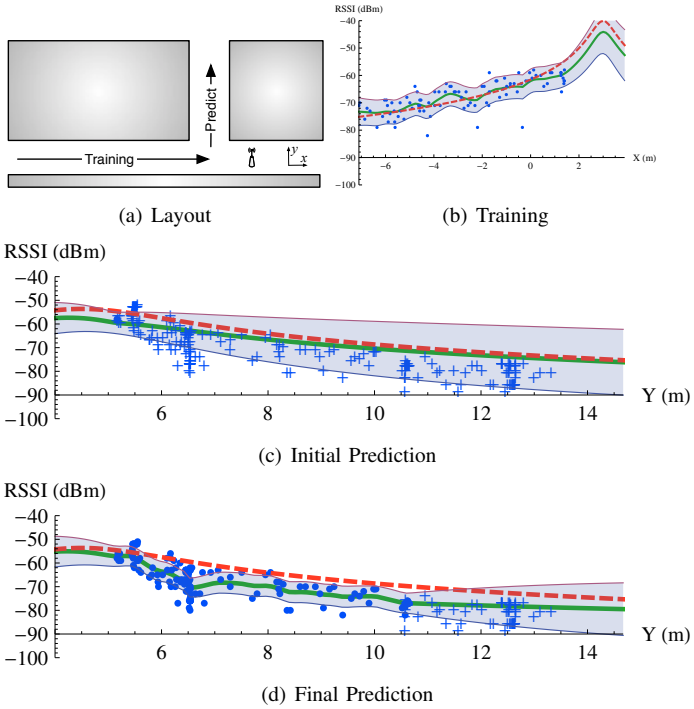

(a) Layout (b) Training

(c) Initial Prediction

(d) Final Prediction

Fig. 7. In a complex hallway environment, we forgo active control due to environmental constraints and instead drive as depicted in Fig. 7(a). Figure 7(b) depicts the training process for the hallway along the x-direction which yields a signal strength prediction as compared to experimental data in Fig. 7(c). Finally, Fig. 7(d) shows how the incorporation of experimental data corrects the prediction.

ACKNOWLEDGEMENTS

We thank both Nathan Michael and Brian Sadler for numerous discussions in the development of this work. We gratefully acknowledge support from: NSF grant no. IIS-0427313, ARO grant no. W911NF-05-1-0219, ONR grants no. N00014-07-1-0829 and N00014-08-1-0696, and ARL grant no. W911NF-08-2-0004.

REFERENCES

[1] XBee®& XBee-Pro® 802.15.4 OEM RF Modules. http://www.digi.com/products/wireless/point-multipoint/xbee-series1-modulespecs.jsp.

[2] M. Abt and W.J. Welch. Fisher information and maximum-likelihood estimation of covariance parameters in Gaussian stochastic processes. *The Canadian Journal of Statistics/La Revue Canadienne de Statistique*, pages 127–137, 1998.

[3] A. Brooks, A. Makarenko, and B. Upcroft. Gaussian process models for sensor-centric robot localisation. In *Robotics and Automation, 2006. ICRA 2006. Proceedings 2006 IEEE International Conference on*, pages 56–61, 2006.

[4] L. Csató. *Gaussian Process: iterative sparse approximations*. PhD thesis, University of Aston in Birmingham, 2002.

[5] E. Damosso, editor. *Digital Mobile Radio: COST 231 View on the Evolution towards 3rd Generation Systems*. The European Comission, 1998.

[6] B. Ferris, D. Fox, and N. Lawrence. Wifi-slam using gaussian process latent variable models. In *Proceedings of the 20th International Joint Conference on Artificial Intelligence (IJCAI 2007)*, pages 2480–2485, 2007.

[7] B. Ferris, D. Hahnel, and D. Fox. Gaussian processes for signal strength-based location estimation. In *Robotics: Science and Systems*, Philadelphia, PA, August 2006.

[8] J. Fink, N. Michael, A. Kushleyev, and V. Kumar. Experimental characterization of radio signal propagation in indoor environments with application to estimation and control. In *Proc. of the IEEE Int. Conf. on Intelligent Robots and Systems*, St. Louis, MO, October 2009. Submitted.

[9] J. M. Gorce, K. Jaffres-Runser, and G. de la Roche. Deterministic approach for fast simulations of indoor radio wave propagation. *IEEE Transactions on Antennas and Propagation*, 55(3):938–948, March 2007.

[10] B. Grocholsky, A. Makarenko, T. Kaupp, and H.F. Durrant-Whyte. Scalable control of decentralised sensor platforms. *Information Processing in Sensor Networks: 2nd Int Workshop*, pages 96–112, 2003.

[11] B. Grocholsky, E. Stump, P. Shiroma, and V. Kumar. Control for localization of targets using range-only sensors. In *Proc. of the International Symposium on Experimental Robotics*. Springer, 2006.

[12] A. Howard, S. Siddiqi, and G. S. Sukhatme. An experimental study of localization using wireless ethernet. In *Field and Service Robotics*, volume 24 of *Springer Tracts in Advanced Robotics*, pages 145–153. Springer Berlin, July 2006.

[13] A. Krause and C. Guestrin. Nonmyopic active learning of Gaussian processes: an exploration-exploitation approach. In *Proceedings of the 24th international conference on Machine learning*, pages 449–456. ACM New York, NY, USA, 2007.

[14] A. M. Ladd, K. E Bekris, A. Rudys, L. E. Kavraki, and D. S. Wallach. Robotics-based location sensing using wireless ethernet. In *Proc. of ACM Int. Conf. on Mobile Computing and Networking*, pages 227–238, Atlanta, GA, September 2002.

[15] N. Lawrence, M Seeger, and R. Herbrich. Fast sparse gaussian process methods: The informative vector machine. *Advances in Neural Information Processing Systems*, 15:625–632, 2003.

[16] S. Martinez, F. Bullo, J. Cortes, and E. Frazzoli. On synchronous robotic networks, part i: Models, tasks and complexity notions. In *Proc. of the IEEE Conf. on Decision and Control*, pages 2847–2852, Seville, Spain, December 2005.

[17] N. Michael, M. M. Zavlanos, V. Kumar, and G. J. Pappas. Maintaining connectivity in mobile robot networks. In *Int. Symposium on Experimental Robotics*, Athens, Greece, July 2008.

[18] C.E. Rasmussen and C.K.I. Williams. *Gaussian processes for machine learning*. Springer, 2006.

[19] E. Snelson and Z. Ghahramani. Sparse Gaussian processes using pseudo-inputs. *Advances in Neural Information Processing Systems*, 18:1257, 2006.

[20] C. Stachniss, C. Plagemann, A. Lilienthal, and W. Burgard. Gas distribution modeling using sparse gaussian process mixture models. In *Proc. of Robotics: Science and Systems (RSS)*, 2008.

[21] G. Wolfle, P. Wertz, and F. M. Landstorfer. Performance, accuracy and generalization capability of indoor propagation models in different types of buildings. In *IEEE Int. Symposium on Personal, Indoor, and Mobile Radio Communications*, Osaka, Japan, September 1999.